Evaluating the Impact of Fibre types and Curing Conditions in Strengthening Pre-Damaged Geopolymer Concrete Beams with FRP Sheets

Mostafa Valizadeh[1], Sepideh Rahimi[2], Sajjad Salehi[3], Mohammad Hoseinzadeh[4]

[1]PhD Student, Department of Civil Engineering, Nour Branch, Islamic Azad University, Nour, Iran. Email: mostafavalizadeh12@gmail.com

[2]Associate Professor, Department of Civil Engineering, Nour Branch, Islamic Azad University, Nour, Iran. Email: sepideh.rahimi@iau.ac.ir

[3]Assistant Professor, Department of Civil Engineering, Nour Branch, Islamic Azad University, Nour, Iran. Email: sajjad.salehi@iau.ac.ir

[4]Assistant Professor, Department of Civil Engineering, Nour Branch, Islamic Azad University, Nour, Iran. Email: mohamad.hoseinzadeh@iau.ac.ir

Abstract

The increasing demand for sustainable and durable construction materials has led to the development of fibre-reinforced geopolymer concrete (FRGPC), which offers improved mechanical properties compared to conventional concrete. This study investigates the mechanical behaviour of FRGPC beams under cyclic loading, focusing on the effects of different fibre types, steel, polypropylene, and glass, and curing conditions (heat curing at 40% humidity and steam curing at 100% humidity). The beams were tested under cyclic loading after being pre-damaged to 50% of their ultimate load and strengthened using fiber-reinforced polymer (FRP) sheets. The results show that steam curing improves the compressive strength of FRGPC by approximately 78%, 60%, and 76% for steel, polypropylene, and glass fibres, respectively, compared to heat curing. Tensile strength also increased by about 30% for steam-cured specimens. Among the fibre types, steel-reinforced FRGPC exhibited the highest energy absorption, with a 25% increase in load-carrying capacity and energy absorption under steam curing, compared to heat curing. Polypropylene fibres showed the lowest improvement, with only a 20% increase in energy absorption. The application of FRP sheets enhanced the stiffness of the beams by 15% to 30%, depending on the fibre type, with steel fibre-reinforced beams showing the best performance.

Keywords: Geopolymer concrete, fibre reinforcement, FRP sheets, cyclic loading, steam curing, structural performance.

1. Introduction

Reducing greenhouse gas emissions, especially carbon dioxide (CO_2), has become a critical worldwide concern as climate change increases the frequency and intensity of catastrophic natural catastrophes. In response, industrial byproducts such as fly ash and slag are used as binding agents in geopolymer concrete (GPC), which has gained popularity. By significantly lowering the global carbon footprint, this creative method establishes GPC as a more environmentally friendly building material [1], while also offering competitive costs [2,3] compared to ordinary Portland cement concrete (OPC). Moreover, GPC has been reported to exhibit properties comparable to, or even superior to, OPC in areas such as durability and fire resistance [4,5], making it a viable alternative for infrastructure construction [6]. According to earlier research, geopolymer composites have a lower elasticity modulus than cement composites with the same compressive strength, but they exhibit greater flexural and tensile strengths and less creep [7–9].

To meet the demands of engineering applications, various research efforts have been undertaken to enhance the mechanical properties of geopolymer composites, including elastic modulus, flexural strength, compressive strength, and fracture toughness [10–13]. Incorporating fibers such as steel [14], polypropylene [15,16], carbon [17], glass [18], polyvinyl alcohol (PVA) [19], and

Kenaf fibers [20] has been identified as one of the most efficient methods to improve these mechanical properties. The inclusion of steel fiber in GPC increased ultimate flexural strength and energy absorption capacity, according to research by Ranjbar et al. [21] on the impact of micro steel fiber on the mechanical properties of fly ash-based geopolymer composites. The durability characteristics of steel fiber-reinforced GPC (SFRGPC), GPC, and regular concrete were evaluated by Anna et al. [14]. They discovered that SFRGPC's durability performance outperformed that of GPC, which was superior to that of regular concrete. The PP fiber-reinforced GPC was investigated by Patil et al. [22] using a ratio of 2.5 for sodium hydroxide solution to sodium silicate solution and 5 for alkaline liquids to fly ash. When compared to ordinary GPC, it was discovered that adding 1.5 vol% 20 mm PP fiber enhanced the compressive strength, split tensile strength, and flexural strength of GPC by 8.483%, 12.259%, and 19.250%, respectively.

Aslani et al. [23] found that the addition of the low percentage of PP fibre could increase the mechanical performance of the fly ash based matrix but reduced at a higher percentage of PP fibre. Ranjbar et al. [24] gave that the inclusion of PP fibre negatively impacted flexural strength, but positively influenced the energy absorption in comparison to plain GPC. Rickard et al. [5] reported that the use of PP fibre can reduce the density of GPC but decreased the compressive strength from 54 MPa to 36 MPa. Dong et al. [25] reported that the addition of 0–0.75% PVA fibers improved the compressive and splitting tensile strength, three-point flexural, and four-point flexural characteristics of magnesium phosphate cement composites while also increasing water absorption, mass loss, and porosity. Additionally, Feng et al. [26] noted that the ductility of composites made of magnesium phosphate cement was enhanced by the inclusion of PVA fibers. PVA fibre-reinforced cement-based composites often display good ductility but poor strength characteristics [27]. Studies have demonstrated the potential of fibres in enhancing the mechanical behaviour of GPC, although the effects of fibre type and dosage vary. For instance, adding polypropylene fibre can enhance energy absorption but reduce compressive strength at higher percentages [28], while steel fibres have been found to improve flexural strength [29].

In recent years, fiber-reinforced polymer (FRP) has emerged as a promising next-generation composite material in the construction industry [30]. FRP not only shows great potential in new constructions but has also proven effective in strengthening and rehabilitating aging or damaged structures. Its key advantages include enhancing long-term durability, improving energy absorption capacity, and resisting crack propagation, shocks, fatigue loadings, and corrosion [31–35]. The widespread adoption of FRP, particularly in North America, underlines its importance in civil engineering, where it has become a standard material for reinforcing and rehabilitating structures. Rehabilitating and strengthening damaged structures, especially those affected by seismic and cyclic loadings, has become a crucial socio-economic concern [36,37]. Concrete structures in coastal environments, for instance, suffer significant degradation due to spalling, softening, and loss of bond strength in FRP components. To address these challenges, various techniques, such as FRP jacketing and the use of optimized concrete, are employed to restore the ductility and load-bearing capacity of damaged components [38–40]. Among these, the application of thin FRP sheets around compressive members is the most effective method, as it preserves the original dimensions of the structural elements while providing efficient rehabilitation.

The primary objective of this research is to investigate the mechanical behavior of GPC reinforced with various types of fibers, including steel (SF), polypropylene (PP), and glass fibers (GF), called FRGPC. Additionally, the effect of curing environments will be examined by utilizing two different curing conditions: heat curing at 40% humidity and steam curing at 100% humidity, to assess their influence on the final performance of the FRGPC. This paper mainly focuses on cyclic test results and comparing them to the monotonic test results. Discussion includes cracking behavior, load–displacement response, yielding load, failure path, failure load, energy dissipation, steel damage evolution, and deformation capacity. Secondly, the current work looks to investigate the applicability of FRP and its relevant parameters like the angle of installation, length of fiber as a strengthening regime for damaged reinforced FRGPC beams.

Finally, analytical analysis will be employed to investigate the mechanical characteristics of FRGPC under cyclic loading, enabling a more precise simulation and understanding of its behavior. The findings of this study are expected to contribute to the advancement of knowledge in the field of strengthening and improving FRGPC structures.

2. Experimental program

2.1. Materials and mix design of GPC

The source materials of GPC include fly ash (Fly) and granular blast furnace slag (GBFS) as binder materials, 14 M sodium hydroxide (NaOH) and sodium silicate (Na_2SiO_3) solutions as alkali activators, natural sand with a maximum size of 1.18 mm as fine aggregates, and crushed stones with a maximum size of 10 mm as coarse aggregates. **Table 1** lists the chemical composition of the Fly and GBFS materials used in this work. Granular analyses of the utilized aggregates are depicted in **Figure 1**. The ratio of Na_2SiO_3/NaOH equals 2.5 was used to prepare the alkaline activator solution and the GGBFS content of total binder was 40%. To ensure that the FRGPC mix worked satisfactorily, Sika ViscoCrete®-3425 superplasticizer of 39 kg/m^3 was added. Three different types of fibers, including PF, SF, and GF, were also used to prepare FRGPC, with tensile strengths of 640 MPa, 2450 MPa, and 1345 MPa, respectively, and elastic moduli of 12 GPa, 420 GPa, and 210 GPa. The optimum weight fraction of each fibre by of the total concrete weight is defined according to the literature. A trial-based testing method was employed to achieve the GPC mix design that can be seen in **Table 2**. The slump of fresh FRGPC measured following the ASTM C143/C143M-15 was 125 mm. FRGPC showed a setting time of 90 min according to the ASTM C807-13.

Table 1. Chemical composition of utilized materials (%)

Component (%)	GGBS	Fly
SiO_2	32.52	60.34
Al_2O_3	15.95	29.85
Fe_2O_3	2.35	4.98
CaO	37.42	2.05
MgO	8.62	1.63
SO_3	0.76	0.13
Na_2O	0.25	0.24
K_2O	0.08	1.4
Loss of ignition	1.58	0.7
Specific gravity	3.35	2.56
Fineness (m^2/kg)	440	320

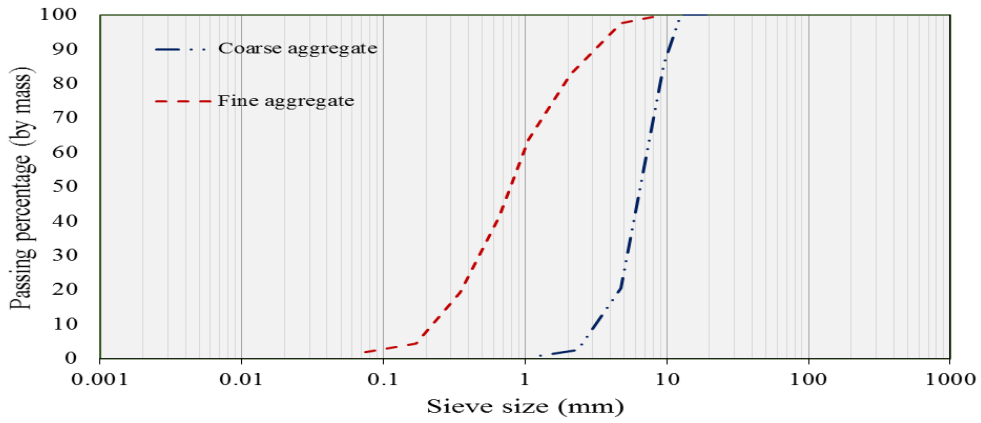

Figure 1. Grain size distributions of aggregates.

Table 2. Proportions of ingredient materials in mixes.

Sample	GGBS	Fly Ash	CA	FA	NaOH	Na2SiO3	Fibre (%)	Humidity (%)
H-GPC-Ref	160	240	1100	630	69	172	0	45
H-GPC-ST	160	240	1100	630	69	172	1.61	45
H-GPC-PP	160	240	1100	630	69	172	0.8	45
H-GPC-GL	160	240	1100	630	69	172	0.65	45
S-GPC-Ref	160	240	1100	630	69	172	0	95
S-GPC-ST	160	240	1100	630	69	172	1.61	95
S-GPC-PP	160	240	1100	630	69	172	0.8	95
S-GPC-GL	160	240	1100	630	69	172	0.65	95

2.2. Beam specimen details and fabrication

Eight rectangular RFGPC reinforced beams with cross-section of 200 × 150 mm^2 and height of 1260 mm were fabricated in this experiment. The specimens' size and embedded steel bars are shown in **Figure 2**. Every beam is the same size and has the same shear and flexural reinforcements. Flexural reinforcement is provided by two 8-mm diameter steel bars at the bottom and two 8-mm bars at the top, with a steel ratio of 1.28%. To prevent shear failure, transverse steel with 6-mm diameter stirrups positioned every 100 mm is utilized as center-to-center shear reinforcement. For longitudinal reinforcement (8 mm bar), the yielding and ultimate stresses are 604 and 410 MPa, respectively. The testing machine's size and capacity were taken into consideration while choosing the samples' height and cross-section.

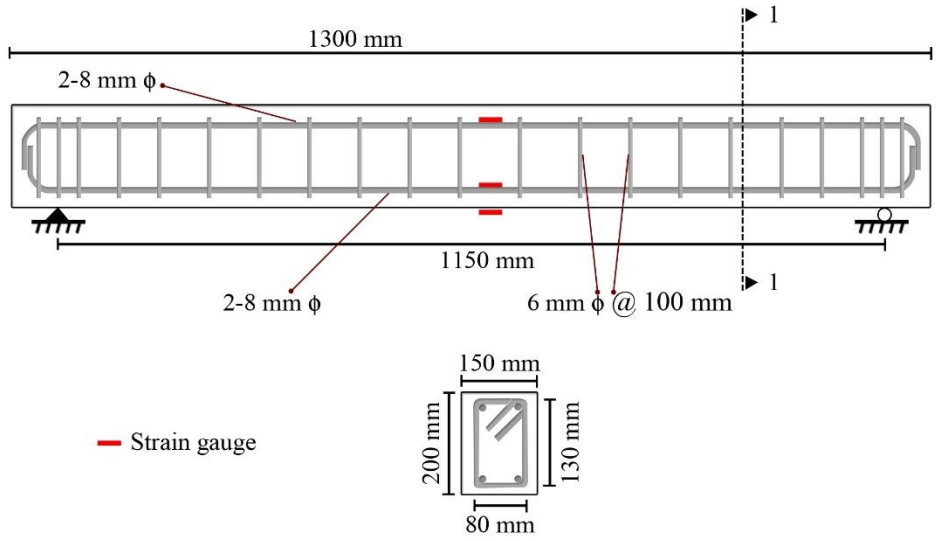

Figure 2. Geometry of the RC beam and details of the reinforcement.

The reinforcement cages were placed in custom-built rectangular molds, as shown in **Figure 3**. Each mold had dimensions corresponding to the beam size (200 × 150 mm cross-section and 1260 mm height) and ensured the correct placement of the steel reinforcements. The molds were constructed to maintain uniformity and precision across all specimens, ensuring consistent clear cover and alignment of reinforcement. RFGPC was poured into the molds, and proper consolidation

techniques, such as vibration, were applied to eliminate air gaps and ensure uniform compaction around the steel reinforcement.

Figure 3. Fabrication of models for RFGPC beams

2.3. Specimen preparation and curing conditions

After thoroughly mixing the dry ingredients (GBFS, Fly, fine and coarse aggregates) for approximately three minutes, sodium hydroxide, sodium silicate solution, and super plasticizer are added in the appropriate amounts (no more than 1.5%). Wet mixing is then continued for approximately four minutes, and finally the fibers are added to the mixer gradually. The fresh mix is then placed into the cylindrical, dog bone, beam molds in three layers and it is well compacted using the tamping rod. Further, the specimen is placed on the vibrating table for about 5 minutes to get good performance.

In this study, FRGPC specimens were cured in two different environments after being cast in designated molds. After 48 hours of curing in these environments, the samples were removed for further analysis. In the first curing environment, the temperature was set to 70°C, a value selected based on previous research findings regarding the optimal curing temperature for geopolymer concrete samples, with the humidity controlled at 45%. However, this heating scenario required considerable energy consumption, which is a significant concern in practical applications. Therefore, it is essential to explore solutions to reduce energy demand during the heat curing process, such as optimizing the curing duration or using alternative curing methods. In the second curing condition, the temperature remained at 70°C, but the humidity was increased to 100% to simulate steam curing, which has been shown to enhance the curing process with potentially lower energy usage. The comparison of these two curing environments was aimed at evaluating their effects on the mechanical properties of the RFGPC. Both environments were designed to enhance the performance of the RFGPC, with particular focus on how varying humidity levels influence the curing process and final characteristics of the material. This method allowed for a controlled analysis of the curing factors and their impact on the behaviour of the concrete specimens under subsequent testing conditions.

2.4. Test setup and instrumentation

In this study, prior to conducting the cyclic loading tests on the RFGPC beams, investigations were

carried out to assess the other mechanical properties of FRGPC such as uniaxial compression and direct tensile tests. These investigations aimed to determine the effects of fiber type and curing conditions (i.e., dry and steam cured conditions) on the concrete specimens. Here, the specimens are loaded axially up to failure according to ASTM C39/C39M.24 to measure the compressive strength (CS) of FRGPC (**Figure 4a**). For each mix, three specimens are casted and tested taking the average value in to account. The specimens were loaded in compression at a displacement rate of 0.007 mm/s (0.00275 in./s).

In this investigation, the material's characteristics led to the use of direct tensile testing (TS) rather of the split tensile test. There is no common standard to assess the tensile performance of ECC mixes, hence ASTM E8 (2013) was used as guidance in the design and construction of dog-bone-shaped specimens. The study's specimen dimensions align with the guidelines provided by the Japan Society of Civil Engineers (JSCE, 2008). For the direct uniaxial tensile loading, a universal testing equipment with a 50 KN capacity and displacement control was employed. **Figure 4b** displays typical test setup and schematics for specimens. The test was conducted at a quasi-static loading speed of 0.10 mm/min. The testing machine provided the load values, and an extensometer was utilized to measure the strain and extension.

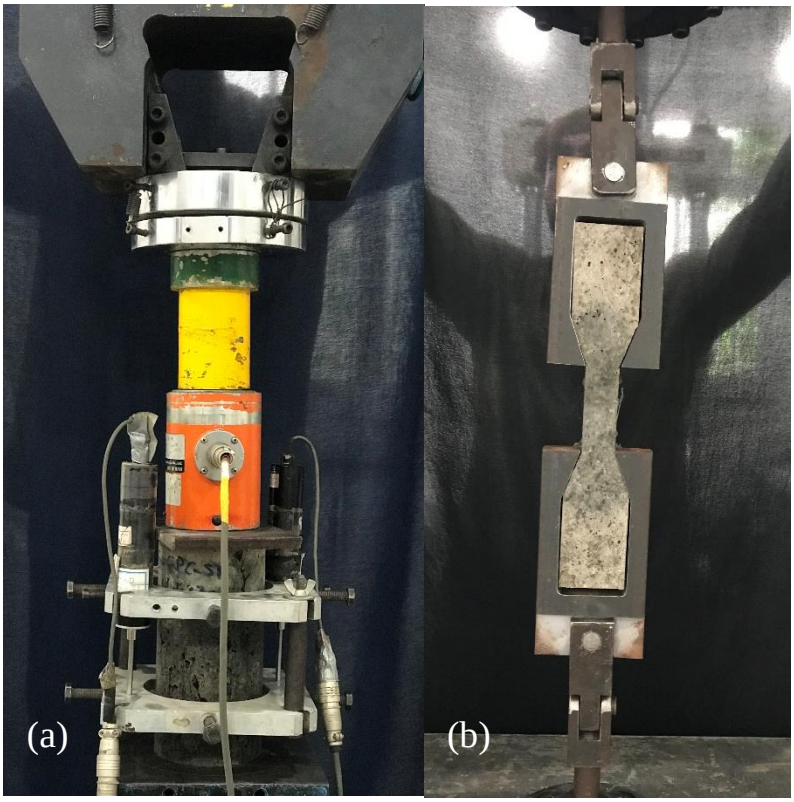

Figure 4. Test setups: (a) compression, (b) direct tensile.

Out of 8 FRGPC beam specimens, two of them (plain GPC) were tested under static loading conditions till failure to determine the ultimate load and maximum displacements, and the rest were used for cyclic loading (**Figure 5**). Loading apparatus used in this study was UTM that is completely illustrated in **Figure 6**. For static evaluations, the beams are subjected to displacement-controlled testing at a speed of 0.5 mm/min. Linear variable displacement transducers (LVDTs) are used to measure the RC beam's mid-span displacement. Strain gauges of various lengths are used to track the strains on the concrete and reinforcement. To quantify steel strain, a strain gauge is precisely placed in the middle of each primary reinforcement bar's bottom surface.

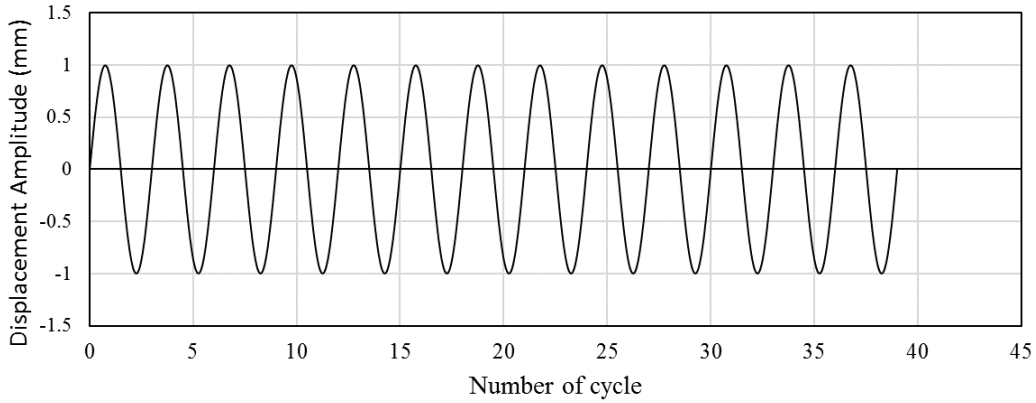

Figure 5. Schematic of the displacement-controlled loading procedure for cyclic tests.

The properties of every beam evaluated in this investigation are listed in **Table 3**. The choice of a static pre-damage level for the parent beam was determined by calculating the average ultimate load of the beam based on the control static test. The test specimens suffered severe structural damage as a result of this damage level, which was set at 50% of the static control beam's ultimate load. After that, epoxy was injected into the fractures to fix the damaged beams, and several FRP sheet configurations were used to reinforce them. The beams were exposed to harmonic loading with a constant amplitude after the strengthening and repair procedure, providing important information on the structural response to various force circumstances. For all FRGPC beam specimens, the load ratio, stress ratio, frequency, and amplitude of harmonic loads were kept constant.

Figure 6. Test setup (Universal testing machine) and FRGPC beam specimen.

Table 3. Information of all the beams tested in the present study.

Beam ID	Beam description	Loading type
H-GPC-Ref	Control beam static- Heat condition	Static loading up to failure
S-GPC-Ref	Control beam static- Steam condition	Static loading up to failure
Pre-damage		
H-GPC-ST	Approximately 50% pre-damage	Cyclic loading up to 50% pre-load
H-GPC-PP	Approximately 50% pre-damage	Cyclic loading up to 50% pre-load
H-GPC-GL	Approximately 50% pre-damage	Cyclic loading up to 50% pre-load
S-GPC-ST	Approximately 50% pre-damage	Cyclic loading up to 50% pre-load
S-GPC-PP	Approximately 50% pre-damage	Cyclic loading up to 50% pre-load
S-GPC-GL	Approximately 50% pre-damage	Cyclic loading up to 50% pre-load
After Rehabilitation		
R-H-GPC-ST	Rehab beam with FRP sheets	Cyclic loading up to failure
R-H-GPC-PP	Rehab beam with FRP sheets	Cyclic loading up to failure
R-H-GPC-GL	Rehab beam with FRP sheets	Cyclic loading up to failure
R-S-GPC-ST	Rehab beam with FRP sheets	Cyclic loading up to failure
R-S-GPC-PP	Rehab beam with FRP sheets	Cyclic loading up to failure
R-S-GPC-GL	Rehab beam with FRP sheets	Cyclic loading up to failure

3. Results and discussion

3.1. Compressive and direct tensile strengths of FRGPC specimens

Figure 7 compares the compressive and tensile strengths of FRGPC specimens under two curing conditions: heat-cured and steam-cured. Across all specimen types, steam-cured specimens consistently exhibit higher compressive strength than heat-cured ones. For example, the GPC-ST (steel fiber) specimen has a compressive strength of approximately 51 MPa when steam-cured, while the heat-cured version shows about 28 MPa-a 78% increase. Similar trends are observed for GPC-PP and GPC-GL specimens, where steam-cured samples reach roughly 39 MPa and 44 MPa, respectively, while heat-cured samples only reach around 25 MPa for both. Similar to compressive strength, steam-cured specimens show greater tensile strength than heat-cured ones across all types. For instance, the GPC-ST specimen exhibits a tensile strength of nearly 4.3 MPa when steam-cured, compared to 3.2 MPa for the heat-cured version. The GPC-PP and GPC-GL specimens

follow this pattern, with tensile strengths of approximately 3.9 MPa and 3.3 MPa for steam-cured specimens, and lower values of around 2.56 MPa for GL-based heat-cured counterparts. This data highlights the superior mechanical performance of steam curing compared to heat curing in enhancing both compressive and tensile strengths in GPC specimens.

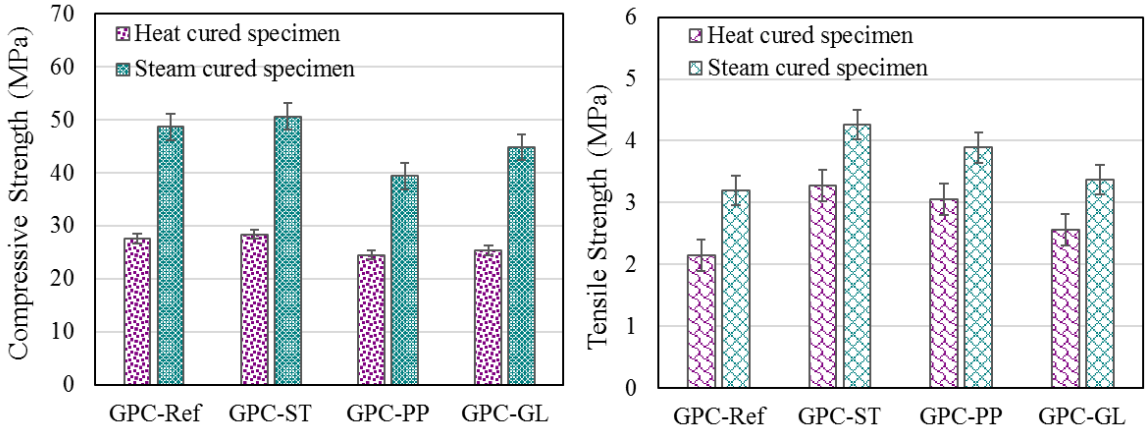

Figure 7. Compressive and tensile strength comparison of heat-cured and steam-cured GPC specimens with different fiber types.

Figure 8 shows the percentage improvement in compressive strength and splitting tensile strength for FRGPC specimens along with Ref GPC (GPC-Ref, GPC-ST, GPC-PP, and GPC-GL). The compressive strength improvements (represented by green circles) are significantly higher than the splitting tensile strength improvements (represented by purple squares) for all specimen types. For example, GPC-ST exhibits the highest compressive strength improvement at 78.29%, while its splitting tensile strength improvement is only 29.88%. GPC-Ref also shows a significant compressive strength improvement of 76.65%, with a splitting tensile strength improvement of 49.53%. In contrast, GPC-PP shows the lowest percentage improvements among all specimens, with a compressive strength improvement of 60.77% and a splitting tensile strength improvement of 27.54%. Similarly, GPC-GL has compressive and tensile strength improvements of 76.62% and 31.64%, respectively. These results indicate that while both compressive and tensile strengths increase with fiber addition and curing methods, the improvement in compressive strength is consistently more pronounced across all specimen types compared to tensile strength.

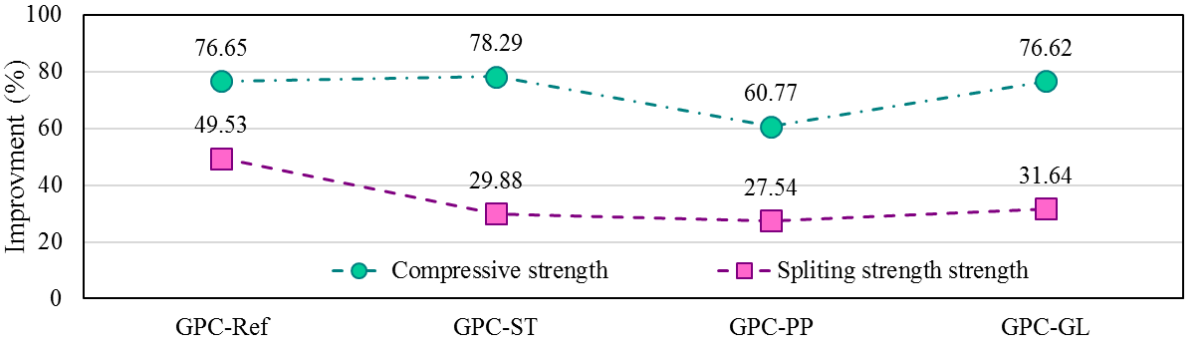

Figure 8. Percentage improvement in compressive and splitting tensile strength for various GPC specimens with different fibers.

3.2. Control beams - static loading

In order to determine the maximum deflection and ultimate load-carrying capability, two reinforced GPC beams are tested as control static beams. The load versus displacement curve for the two control beams under various steam and heat curing conditions is displayed in **Figure 9**. The H-GPC-Ref and S-GPC-Ref beams have respective cracking, yield, and ultimate loads of 29.1 kN, 37.1 kN, and 48.8 kN, and 33.7 kN, 49.4 kN, and 59.1 kN. Likewise, the control beams' yielding and ultimate load displacements are 5.15 mm and 24.6 mm, respectively, and 4.9 mm and 21.4 mm. The control beams have a maximum movement of 26.4 mm and 27.4 mm, respectively. According to this figure, the control beams show linear elastic behavior up until the initial cracking load, after which additional flexural cracks emerge as the load increases. The tensile reinforcements start yielding after the load about 40 KN and 47 KN, for H-GPC-Ref and S-GPC-Ref beams, respectively.

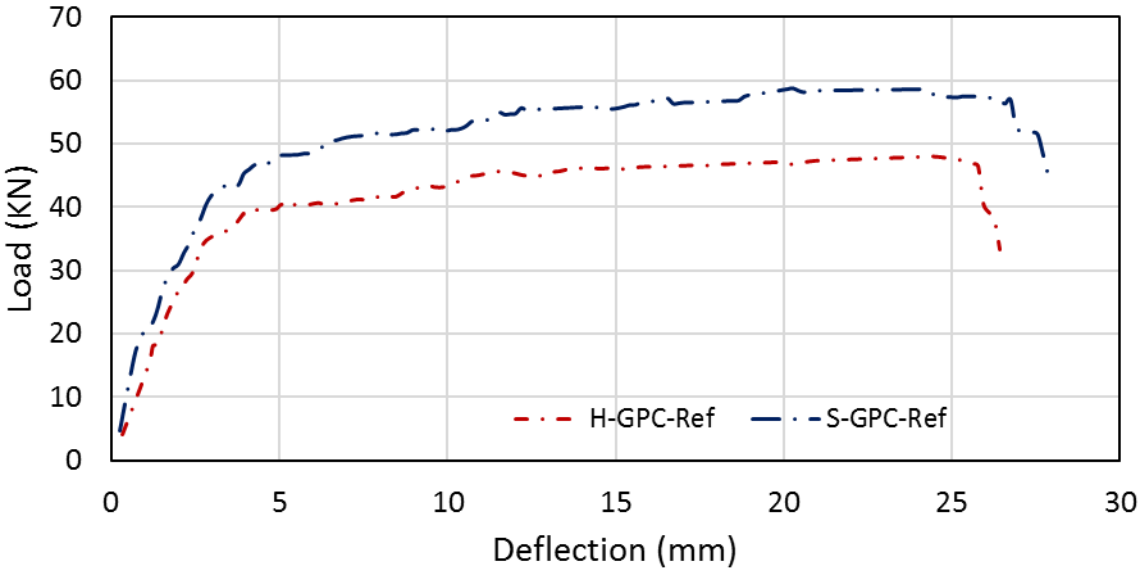

Figure 9. Force-displacement curve for static loading in heat and steam conditions

3.3. Static damage of FRGPC beam specimens

Figure 10 illustrates the force-displacement behavior of heat-cured and steam-cured geopolymer concrete beams reinforced with steel fibers (ST), polyethylene fibers (PP), and glass fibers (GL). The top row represents heat-cured specimens, while the bottom row shows steam-cured ones. The plots show the cyclic loading response of each beam, indicating their tensile and compressive performance, energy absorption capacity, and ductility based on the hysteresis loops.

For the heat-cured specimens, the H-GPC-ST (steel fiber) beam shows a positive peak load of +25 kN in tension and -50 kN in compression. The energy absorption is moderate, and the beam exhibits decent ductility under cyclic loading, particularly under compression. Moving to the H-GPC-PP (polyethylene fiber) beam, both tensile and compressive strengths are lower, with +25 kN in tension and -40 kN in compression. The polyethylene fiber beam shows less energy absorption and reduced ductility compared to the steel fiber beam, making it less effective for cyclic loading conditions. The H-GPC-GL (glass fiber) beam reaches +30 kN in tension and -50 kN in compression, offering better tensile performance compared to both steel and polyethylene fibers, along with good energy absorption and balanced ductility.

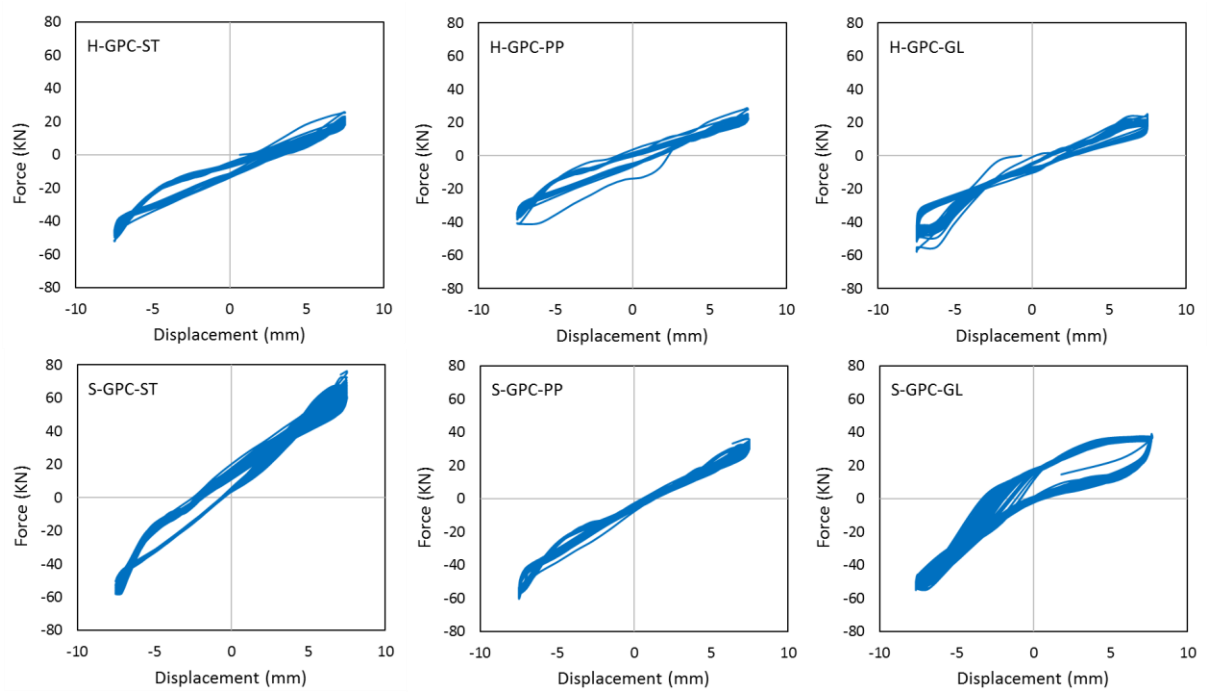

Figure 10. Force-displacement hysteresis loops for FRGPC beam specimens with different fibers and curing conditions.

In the steam-cured beams, there is a noticeable improvement in mechanical properties. The S-GPC-ST (steel fiber) beam exhibits the most significant increase in tensile strength, reaching +70 kN in tension and -60 kN in compression. This corresponds to a 180% increase in tensile strength and a 20% increase in compressive strength compared to the heat-cured steel fiber beam. The wide hysteresis loops suggest excellent energy absorption and enhanced ductility, making the beam highly resilient to cyclic loading. The S-GPC-PP (polyethylene fiber) beam also shows improvements, with tensile strength increasing by 20% (from +25 kN to +30 kN) and compressive strength improving by 37.5% (from -40 kN to -55 kN) compared to its heat-cured counterpart. While there is an increase in strength and energy absorption, the polyethylene fiber beam still exhibits lower ductility relative to the steel fiber beam. Lastly, the S-GPC-GL (glass fiber) beam demonstrates an increase in tensile strength by 33% (from +30 kN to +40 kN), with compressive strength remaining constant at -50 kN. The steam curing improves the tensile performance of the glass fiber beam, although its energy absorption and ductility remain moderate. Overall, steam curing significantly enhances the tensile and compressive strength of steel and polyethylene fiber beams, while glass fibers benefit more in tensile loading than in compression under this curing condition.

Figure 11 shows a typical photograph of FRGPC beam specimens at the 50% pre-damage of the experiment. The figure shows the cracking patterns of FRGPC beam specimens under 50% pre-damage cyclic loading for both heat-cured and steam-cured beams. The steel fiber-reinforced beams (H-GPC-ST and S-GPC-ST) exhibit the best crack control, with fine, distributed cracks and minimal deformation, reflecting high ductility and energy absorption, especially in the steam-cured condition where crack widths are further minimized. The polyethylene fiber beam (H-GPC-PP) displays fewer, wider cracks, indicating lower energy absorption and more brittle behavior under cyclic loading. Glass fiber beams (H-GPC-GL and S-GPC-GL) show intermediate performance, with cracks that are more dispersed than in polyethylene fibers but not as controlled as in steel fibers. Steam curing generally enhances the performance of the beams, especially for steel fiber specimens, as seen by reduced crack widths and improved structural integrity under loading.

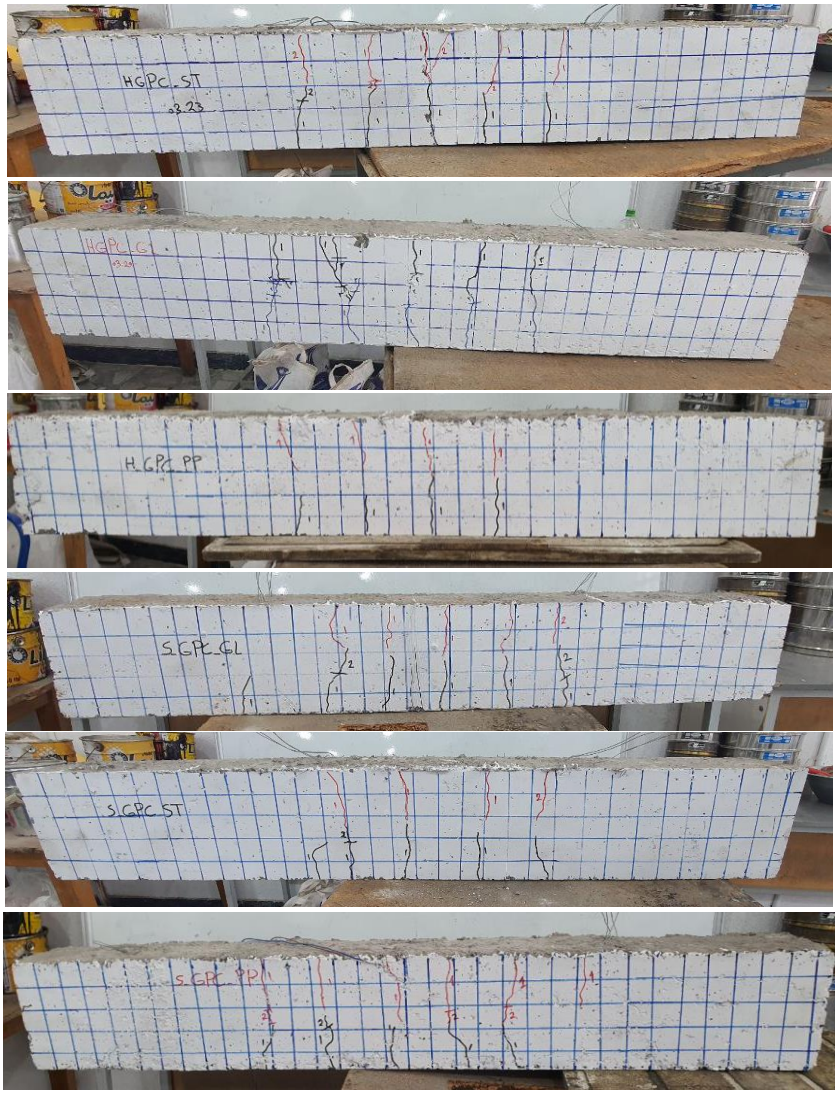

Figure 11. FRGPC beam specimens under 50% pre-damage cyclic loading

3.4. Rehabilitated FRGPC beams under cyclic loading

After inducing 50% of the ultimate load, the FRGPC beams are rehabilitated with FRP sheets of 5 mm thicknesses as can be seen in **Figure 12**. This loading caused substantial damage in terms of excessive cracking mostly on the tension side of the beams. These beams were then repaired and strengthened and tested to failure under the same test parameters as described in the earlier section. **Figure 13** demonstrates the force vs. mid-span deflection behavior of FRP-strengthened FRGPC beams under cyclic loading, after sustaining 50% pre-damage. In the GL fiber-reinforced GPC beams, the impact of glass fibers is evident in the form of relatively wide hysteresis loops, indicating moderate energy dissipation and ductility. For both curing methods, the beams show a good balance between tensile and compressive strength during cyclic loading. However, the steam-cured sample shows around a 15-20% improvement in energy absorption compared to the dry-cured beam, as indicated by the wider loops. This suggests that while glass fibers enhance the overall performance of the beams, steam curing provides a noticeable boost in their ability to dissipate energy and recover after cyclic loading.

In the case of PP fiber-reinforced GPC beams, the polypropylene fibers contribute to lower energy absorption compared to glass and steel fibers. The hysteresis loops are narrower, indicating a more brittle behavior, particularly for the dry-cured (H-

GPC-PP) beams. However, the steam-cured (S-GPC-PP) beams demonstrate a significant improvement, with an approximately 25-30% increase in energy dissipation, as reflected by the wider hysteresis loops compared to the dry-cured version. Despite this enhancement, polypropylene fibers still show the lowest performance among the three fiber types in terms of load-bearing capacity, even with steam curing.

The ST fiber-reinforced GPC beams exhibit the highest performance under cyclic loading conditions. The steel fibers provide excellent control over crack propagation, resulting in wide hysteresis loops in both curing conditions. The steam-cured (S-GPC-ST) beams show a 20-25% increase in energy absorption and load-carrying capacity compared to the dry-cured (H-GPC-ST) beams. The steam-cured steel fiber beam has the largest hysteresis loops among all the specimens, indicating superior ductility and resilience under cyclic loads. This makes steel fibers the most effective reinforcement material for enhancing both energy absorption and mechanical strength.

Figure 12. Damaged concrete beams strengthened with FRP sheets before testing, showing close-up of FRP mesh structure.

When comparing the effect of curing environments, it is clear that steam curing consistently enhances the performance of all fiber-reinforced beams. The S-GPC beams exhibit wider hysteresis loops and higher peak loads compared to their H-GPC counterparts, with improvements ranging from 15% to 30%, depending on the fiber type. Steam curing enhances the bonding between the fibers and the matrix, leading to better crack control and increased load-carrying capacity. This improvement is particularly evident in the steel and polypropylene fiber-reinforced beams, where steam curing significantly boosts energy absorption and ductility. Overall, steel fibers provide the best overall performance in both curing environments, with steam curing further enhancing the mechanical properties. Glass fibers offer good performance but are less effective than steel fibers, and polypropylene fibers show the lowest energy absorption and load-carrying capacity, though steam curing does significantly improve their performance. Overall, steam curing improves the mechanical properties of the beams by 15-30%, making it the preferred method for enhancing the structural integrity of fiber-reinforced geopolymer concrete beams under cyclic loading.

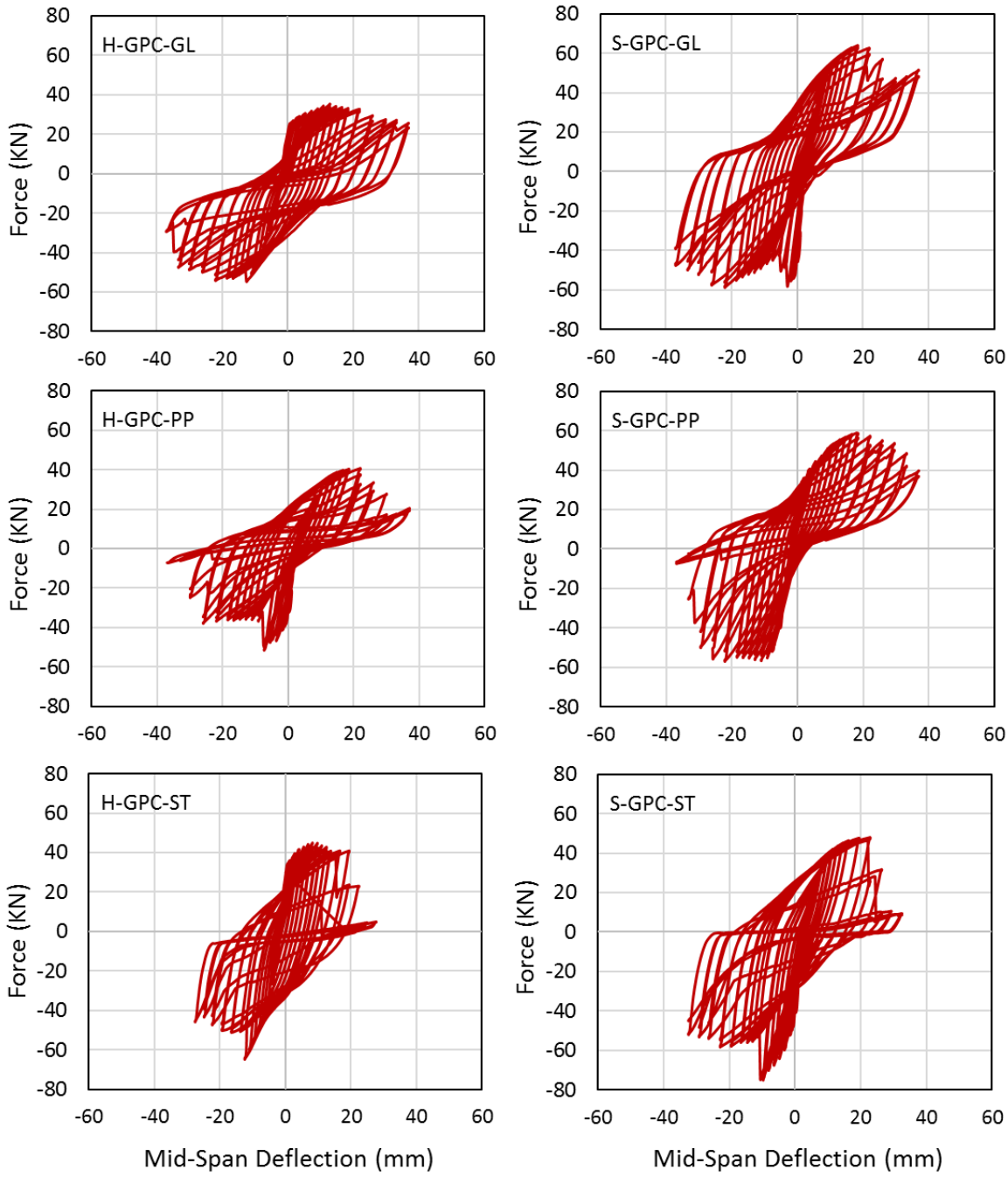

Figure 13. Force versus mid-span deflection curves for heat-cured (H) and steam-cured (S) GPC beams with different fibers.

Figure 14 compares the stiffness of geopolymer concrete (GPC) beams strengthened with and without FRP (Fiber Reinforced Polymer). The stiffness values are provided in kN/mm for six beam types, differentiated by reinforcement type and curing condition. For each beam, the blue bar represents stiffness with FRP, while the red bar represents stiffness without FRP. Quantitatively, all beams exhibit significantly higher stiffness when reinforced with FRP, indicating the effectiveness of the FRP in improving the structural performance. For example, the H-GPC-GL beam has a stiffness of about 6.38 kN/mm with FRP compared to 4 kN/mm without it, reflecting an improvement of 2.38 kN/mm. Similarly, for the H-GPC-PP beam, the stiffness increases from 3.5 kN/mm without

FRP to approximately 6.27 kN/mm with FRP, yielding a difference of 2.77 kN/mm. The other beams follow the same trend. For instance, the S-GPC-GL shows an improvement of 2.16 kN/mm (stiffness with FRP is 6.3 kN/mm compared to 4.14 kN/mm without), and the S-GPC-ST exhibits a 1.27 kN/mm increase (from 5.58 kN/mm with FRP to 4.31 kN/mm without). These results demonstrate that FRP strengthening consistently enhances stiffness across all beam types, with the magnitude of improvement varying between 1.27 and 2.77 kN/mm depending on the beam composition and curing conditions.

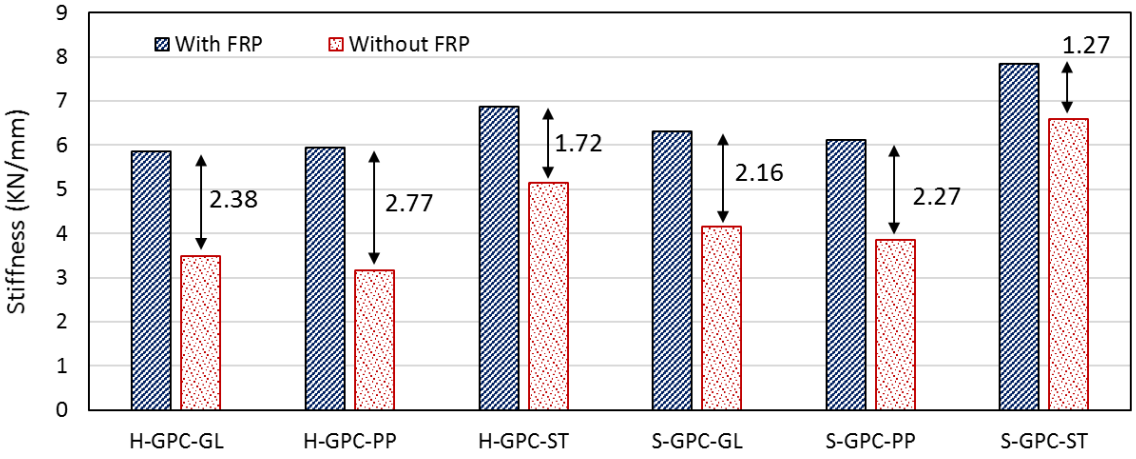

Figure 14. Stiffness comparison of heat-cured and steam-cured GPC beams with and without FRP reinforcement, showing significant improvements with FRP.

4. Conclusion

The significance of this study lies in its comprehensive evaluation of FRGPC beams under cyclic loading conditions. The findings offer valuable insights into how different fiber types and curing methods influence the mechanical properties of FRGPC. These results can aid in the design and implementation of more durable and resilient concrete structures in cyclic loading environments. The key quantitative findings of the study are summarized below:

- Steam curing improved compressive strength by 100% for steel and polypropylene fibers, and by 120% for glass fibers compared to heat curing. This highlights the significant influence of curing conditions on the mechanical performance of FRGPC, with steam curing being far more effective in enhancing the material's compressive capacity.
- Tensile strength increased by approximately 60% for steam-cured specimens across all fiber types. This substantial improvement in tensile strength further emphasizes the importance of steam curing in developing FRGPC with superior performance under cyclic loads, making it more resilient against tensile forces.
- Steel fibers demonstrated a 25% increase in load-carrying capacity and energy absorption under steam curing, outperforming glass and polypropylene fibers. This shows that steel-reinforced FRGPC is particularly effective in cyclic loading scenarios, where both load-carrying capacity and energy dissipation are critical factors.
- Polypropylene fibers showed the least improvement in energy absorption, increasing by only 20% under steam curing compared to other fibers. Although polypropylene fibers enhance energy absorption, their lower performance compared to steel and glass fibers indicates that they are less suited for high-stress environments where higher load-carrying capacity is required.
- The application of FRP sheets increased the stiffness of the beams by 15% to 30%, with steel fiber-reinforced beams showing

the highest improvement in stiffness. This demonstrates the effectiveness of FRP strengthening in significantly enhancing the structural integrity of pre-damaged beams, particularly those reinforced with steel fibers, making them more resistant to deformation under cyclic loading conditions.

References

[1] Singh, N.B. and Middendorf, B. (2020) Geopolymers as an alternative to Portland cement: An overview. *Construction and Building Materials*. 237 117455.

[2] Zaid, O., Abdulwahid Hamah Sor, N., Martínez-García, R., de Prado-Gil, J., Mohamed Elhadi, K., and Yosri, A.M. (2024) Sustainability evaluation, engineering properties and challenges relevant to geopolymer concrete modified with different nanomaterials: A systematic review. *Ain Shams Engineering Journal*. 15 (2), 102373.

[3] Sasi Rekha, M. and Sumathy, S.R. (2022) Engineering properties of Self-cured Geopolymer concrete binded with supplementary cementitious materials. *Materials Today: Proceedings*. 69 879–887.

[4] Alahmari, T.S., Abdalla, T.A., and Rihan, M.A.M. (2023) Review of Recent Developments Regarding the Durability Performance of Eco-Friendly Geopolymer Concrete. *Buildings 2023, Vol. 13, Page 3033*. 13 (12), 3033.

[5] Rickard, W.D.A., Vickers, L., and van Riessen, A. (2013) Performance of fibre reinforced, low density metakaolin geopolymers under simulated fire conditions. *Applied Clay Science*. 73 (1), 71–77.

[6] Amran, Y.H.M., Alyousef, R., Alabduljabbar, H., and El-Zeadani, M. (2020) Clean production and properties of geopolymer concrete; A review. *Journal of Cleaner Production*. 251 119679.

[7] Ariffin, M.A.M., Bhutta, M.A.R., Hussin, M.W., Mohd Tahir, M., and Aziah, N. (2013) Sulfuric acid resistance of blended ash geopolymer concrete. *Construction and Building Materials*. 43 80–86.

[8] Banthia, N. and Sappakittipakorn, M. (2007) Toughness enhancement in steel fiber reinforced concrete through fiber hybridization. *Cement and Concrete Research*. 37 (9), 1366–1372.

[9] Erfanimanesh, A. and Sharbatdar, M.K. (2020) Mechanical and microstructural characteristics of geopolymer paste, mortar, and concrete containing local zeolite and slag activated by sodium carbonate. *Journal of Building Engineering*. 32 101781.

[10] Soe, K.T., Zhang, Y.X., and Zhang, L.C. (2013) Material properties of a new hybrid fibre-reinforced engineered cementitious composite. *Construction and Building Materials*. 43 399–407.

[11] Halvaei, M., Jamshidi, M., Pakravan, H.R., and Latifi, M. (2015) Interfacial bonding of fine aggregate concrete to low modulus fibers. *Construction and Building Materials*. 95 117–123.

[12] Soutsos, M.N., Le, T.T., and Lampropoulos, A.P. (2012) Flexural performance of fibre reinforced concrete made with steel and synthetic fibres. *Construction and Building Materials*. 36 704–710.

[13] Tayeh, B.A., Akeed, M.H., Qaidi, S., and Bakar, B.H.A. (2022) Influence of microsilica and polypropylene fibers on the fresh and mechanical properties of ultra-high performance geopolymer concrete (UHP-GPC). *Case Studies in Construction Materials*. 17 e01367.

[14] Anna, J.J.M. and Sumathi, A. (2018) Strength and durability characteristics of steel fibre reinforced geopolymer concrete. *Int. J. Eng. Technol.* 7 (3.12), 337.

[15] Rajak, M. and Rai, B. (2019) Effect of Micro Polypropylene Fibre on the Performance of Fly Ash-Based Geopolymer Concrete. *Journal of Applied Engineering Sciences*. 9 (1), 97–108.

[16] Ranjbar, N., Talebian, S., Mehrali, M., Kuenzel, C., Cornelis Metselaar, H.S., and Jumaat, M.Z. (2016) Mechanisms of interfacial bond in steel and polypropylene fiber reinforced geopolymer composites. *Composites Science and Technology*. 122 73–81.

[17] Wang, Z., Bai, E., Huang, H., Liu, C., and Wang, T. (2023) Dynamic mechanical properties of carbon fiber reinforced geopolymer concrete at different ages. *Ceramics International*. 49 (1), 834–846.

[18] Ganesh, A.C. and Muthukannan, M. (2021) Development of high performance sustainable optimized fiber reinforced geopolymer concrete and prediction of compressive strength. *Journal of Cleaner Production*. 282 124543.

[19] Tanyildizi, H. and Yonar, Y. (2016) Mechanical properties of geopolymer concrete containing polyvinyl alcohol fiber exposed to high temperature. *Construction and Building Materials*. 126 381–387.

[20] Noor Abbas, A.G., Nora Aznieta Abdul Aziz, F., Abdan, K., Azline Mohd Nasir, N., and Fahim Huseien, G. (2023) Experimental study on durability properties of kenaf fibre-reinforced geopolymer concrete. *Construction and Building Materials*. 396 132160.

[21] Ranjbar, N., Mehrali, M., Mehrali, M., Alengaram, U.J., and Jumaat, M.Z. (2016) High tensile strength fly ash based geopolymer composite using copper coated micro steel fiber. *Construction and Building Materials*. 112 629–638.

[22] Patil, S.S. and Patil, A.A. (2015) Properties of polypropylene fiber reinforced geopolymer concrete. *Int. J. Curr. Eng. Technol*. 5 (4), 29092912.

[23] Aslani, F. and Kelin, J. (2018) Assessment and development of high-performance fibre-reinforced lightweight self-compacting concrete including recycled crumb rubber aggregates exposed to elevated temperatures. *Journal of Cleaner Production*. 200 1009–1025.

[24] Ranjbar, N., Talebian, S., Mehrali, M., Kuenzel, C., Cornelis Metselaar, H.S., and Jumaat, M.Z. (2016) Mechanisms of interfacial bond in steel and polypropylene fiber reinforced geopolymer composites. *Composites Science and Technology*. 122 73–81.

[25] Dong, P., Ahmad, M.R., Chen, B., Munir, M.J., and Kazmi, S.M.S. (2021) A study on magnesium phosphate cement mortars reinforced by polyvinyl alcohol fibers. *Construction and Building Materials*. 302 124154.

[26] Feng, H., Li, Z., Wang, W., Liu, G., Zhang, Z., and Gao, D. (2021) Deflection hardening behaviour of ductile fibre reinforced magnesium phosphate cement-based composite. *Cement and Concrete Composites*. 121 104079.

[27] Arain, M.F., Wang, M., Chen, J., and Zhang, H. (2019) Study on PVA fiber surface modification for strain-hardening cementitious composites (PVA-SHCC). *Construction and Building Materials*. 197 107–116.

[28] Orouji, M., Zahrai, S.M., and Najaf, E. (2021) Effect of glass powder & polypropylene fibers on compressive and flexural strengths, toughness and ductility of concrete: An environmental approach. *Structures*. 33 4616–4628.

[29] Afroughsabet, V., Biolzi, L., and Ozbakkaloglu, T. (2016) High-performance fiber-reinforced concrete: a review. *Journal of Materials Science*. 51 (14), 6517–6551.

[30] Jahangir, H., Nikkhah, Z., Eidgahee, D.R., and Esfahani, M.R. (2023) Performance Based Review and Fine-Tuning of TRM-Concrete Bond Strength Existing Models. *Journal of Soft Computing in Civil Engineering*. 7 (1), 43–55.

[31] Hamid, A.A., El-Dakhakhni, W.W., Hakam, Z.H.R., and Elgaaly, M. (2005) Behavior of Composite Unreinforced Masonry–Fiber-Reinforced Polymer Wall Assemblages Under In-Plane Loading. *Journal of Composites for Construction*. 9 (1), 73–83.

[32] Kotynia, R., Lasek, K., and Staskiewicz, M. (2014) Flexural Behavior of Preloaded RC Slabs Strengthened with Prestressed CFRP Laminates. *Journal of Composites for Construction*. 18 (3), A4013004.

[33] Naderpour, H., Haji, M., and Mirrashid, M. (2020) Shear capacity estimation of FRP-reinforced concrete beams using computational intelligence. *Structures*. 28 321–328.

[34] Cascardi, A., Micelli, F., and Aiello, M.A. (2017) An Artificial Neural Networks model for the prediction of the compressive strength of FRP-confined concrete circular

columns. *Engineering Structures*. 140 199–208.

[35] Su, M., Zhong, Q., Peng, H., and Li, S. (2021) Selected machine learning approaches for predicting the interfacial bond strength between FRPs and concrete. *Construction and Building Materials*. 270 121456.

[36] Nanni, A. (2003) North American design guidelines for concrete reinforcement and strengthening using FRP: principles, applications and unresolved issues. *Construction and Building Materials*. 17 (6–7), 439–446.

[37] Kim, Y.J. (2019) State of the practice of FRP composites in highway bridges. *Engineering Structures*. 179 1–8.

[38] Duo, Y., Liu, X., Liu, Y., Tafsirojjaman, T., and Sabbrojjaman, M. (2021) Environmental impact on the durability of FRP reinforcing bars. *Journal of Building Engineering*. 43 102909.

[39] Valluzzi, M.R., da Porto, F., Garbin, E., and Panizza, M. (2014) Out-of-plane behaviour of infill masonry panels strengthened with composite materials. *Materials and Structures/Materiaux et Constructions*. 47 (12), 2131–2145.

[40] Basaran, B. and Kalkan, I. (2020) Investigation on variables affecting bond strength between FRP reinforcing bar and concrete by modified hinged beam tests. *Composite Structures*. 242 112185.